An Effective Skin Lesion Segmentation in Dermoscopic Images using Optimized Deep Learning Framework

[*1]Ramandeep Kaur

[*1]Department of Computer Science,
Sri Guru Granth Sahib World University, Fatehgarh Sahib, Punjab, 140406, India.
[*]Email: ramancheemachahal@gmail.com

[2]Dr. Navdeep Kaur

[2]Department of Computer Science,
Sri Guru Granth Sahib World University, Fatehgarh Sahib, Punjab, 140406, India
Email: drnavdeep.sggswu@gmail.com

Abstract:

Melanoma is the most threatening type of skin cancer caused by the uncontrolled growth of melanocytes. Analysis of melanoma skin cancer in advance is significant for the better treatment to avoid transferring into other parts of the body. Manual inspections are done by the specialists tends to inaccurate outcomes. The effective role to identify the disease is processed through medical image processing. Segmentation of an image is indulged for extracting precise information of each image pixel with certain characteristics. Computer Aided Diagnosis (CAD) based deep learning technique is applied effectively for the evaluation of different skin conditions using dermoscopic images. Several computational methods are utilised for the exact and rapid identification of the lesion. The proposed method of Deep CNN-OAD (Convolutional neural network-Optimized Adam) comprises the following steps as Pre-processing, Colour enhancement and image segmentation. The input images are pre-processed by Adaptive bilateral filtering and Min-Max normalisation methods in order to remove noises. Afterwards, colour enhancement is done through equalisation of adaptive histogram for upgrading the quality of an image. Finally, Deep CNN-OAD is used for accurately segmenting the lesions. MATLAB is the simulation tool used for predicting the performance of output. The proposed method is examined with the ISIC 2019 dataset. The mean value of various performance metrics are evaluated on the basis of sample comparison. The accuracy rate achieved through segmentation performance is 94.06% in the proposed work.

Keywords: **Filtering, normalization, Color enhancement, Segmentation, Deep learning**.

1. Introduction

The human skin is the outer covering of the body and is the largest organ of integumentary system. Cancer is one of the life-threatening diseases in the world. One of the unbearable types amongst them is skin cancer (SC) [1].The human skin is composed of two major layers as epidermis and dermis. The topmost layer or the outer layer is called the epidermis and the inner layer is called the dermis. The extension of abnormal cells in the outer layer of skin and the unrepaired damage of DNA leads to rapid multiplication of cells which cause tumours [2]. A skin lesion is an abnormal growth or rash on the skin as compared to the normal skin. The two main categories of skin lesion are primary and secondary lesion. Primary skin lesion includes birthmarks, blisters, macules, nodules, papules and pustules. Secondary skin lesion includes crust, ulcer, scales, scar and skin atrophy [3]. The symptoms of skin cancer are a pearly or waxy bump, a flat-flesh coloured lesion, a bleeding sore that heals and returns, a firm, red nodule, a flat lesion with a scaly, crusted surface, a large brownish spot, itches or burns, dark lesions on the palms [4]

The four major types of SC are basal cell carcinoma, Squamous cell carcinoma, merkel cell carcinoma and melanoma. Basal cell carcinoma is the most common non-benign tumour in individuals with fair skin type and it is increasingly seen among the younger patients. Squamous cell carcinoma is a common form of skin cancer that develops in the squamous cells, which make up the middle and outer layers of the skin and it is usually not life threatening, though it can be aggressive. Merkel cell carcinoma is a very rare and extremely aggressive neuro endocrine carcinoma of the skin. The severe type amidst is Melanoma and it occurs in the melanocytes [5]. Melanoma is a tumour of melanin forming cells and it may initiate from an existing mole that changes its size, shape or colour. Late detection of this disease leads to spread of cancer cells to various body parts which affects

© The Author(s) 2023. This is an open access article published under the CC BY license (https://creativecommons.org/licenses/by/4.0/).

liver, lungs and brain and other organs [6]. Melanoma can be further divided into malignant melanoma and Non-malignant melanoma.

Malignant melanoma has a significantly higher morbidity and mortality which results in 65% of deaths from skin cancer. Non-malignant melanoma falls within the most common types being basal cell carcinoma and Squamous cell carcinoma. People get affected by melanoma due to direct flow of UV radiation from sunrays. In addition to radiations, the skin cancer can be attributed to other factors like a history of cancerous genes in the family, hair colour of patients. Hence early diagnosis of melanoma SC has the potential to save a human's life [7]. Dermoscopy is one of the major techniques used for the detection of melanoma, other pigmented skin lesions and to examine the structure of the skin. Due to the difficulties in the human interpretation, computerized analysis of dermoscopy images is playing a vital role. Dermoscopy imaging techniques are used to analyse the deeper level skin lesion and to diagnose the presence of melanoma [8].

The dermatologist conducts visual analysis to catch out various clinical characteristics of melanoma lesion including asymmetry, irregular borders, colour variation, diameter greater than 6mm and the evolving nature of mole. When the dermatologist acquires pigments from the affected area to differentiate the melanoma through visual detection techniques, it complicates the treatment due to insufficient details about the minute artefacts like hairs, clinical marks and colour [9]. However, the data are not sufficient for the exact prediction and the detection accuracy is based on the dermatologist. To conquer over these problems, Melanoma detection and segmentation using CAD based technique is used. CAD plays a key role in upgrading biomedical systems for various applications and helps in the detection, prediction and classification of diseases [10].

The five stages of CAD analysis system are pre-processing, segmentation, feature selection, feature extraction and feature classification [11]. Pre-processing is the preliminary step done to acquire the accuracy by removing the noise, artifacts, inconsistent data through various filters. Segmentation is the process by which the lesion is divided into regions by the surrounding skin based on various properties such as color, texture. The use of segmentation is to provide more information than which exists in medical images. Segmentation method reduces a colour image into an intensity image and segments the image approximately by intensity thresholding. The resulted segments are refined using the image edges. [12]. Feature selection is the process of selecting the reduced input variables to improve the final performance. Feature extraction is the process of conversion of the given input data into a reduced set of features. Feature classification is a recognition technique used to categorize a huge number of data into different classes [13]. The various techniques of machine learning language like support vector machine, decision tree, naïve bayes and k- nearest neighbour has certain drawbacks [14, 15]. Deep learning has captivated a lot of attentions in the medical field. Deep learning technique offers rich responsibility and it is often carried out to bring end to end training in deep applications. The information can be encoded effectively and performs information processing across multiple modality. It generates the outcome of the data analysis in detailed manner and improves diagnosis. Conceivably, it reduces reporting delays and highlights the cases effectively. This is clearly an advantage in CAD based deep learning technique compared to the machine learning technique.

Motivation

The reflections of melanoma cancer have been increasing to a higher extent and there are more chances to get recovered by analysing at the early stage. It can occur on the surface of any type of skin and most commonly found in fair skin. So many difficulties raise due to the differentiated data like position, skin lines and various methods are indulged for the skin lesion segmentation. Because of non-invasiveness, the determination of SC is done in most of the image processing research papers. Segmentation process is widely used and it acts as the fundamental step over here. But, the domain knowledge of diseases, medical imaging modality is needed to guide for feature design and extraction. Hence it leads to time consumption, less accuracy and human intervention is required. For the better result, segmentation method is carried out for the detection of exact disease. To overcome the traditional drawbacks, segmentation using CAD based deep learning technique is applied, as it does not require hand- engineered features. To suppress the issues in previous papers, the proposed method of Deep CNN-OAD is implemented, which offers a powerful diagnostic technique for exact estimation and it is highly beneficial to the doctors.

Contributions

The major contributions of this research are summarized below:

- To introduce an effective method for pre-processing, enhancement of colour, and segmentation of image for the detection of melanoma skin cancer by the use of deep learning model.
- To perform the methods of adaptive bilateral filtering and Min-Max normalisation, the removal of noise is done at the pre-processing step. The visibility of noise is neglected by smoothening the areas of the entire image for the detailed view. Colour enhancement process is carried out by the equalisation of adaptive histogram and the segmentation process is enhanced by the combined algorithm of Deep CNN-OAD.

- To show better accuracy rate in the detection and segmentation of melanoma skin cancer, the deep learning based technique is enhanced.
- To effectively design and develop the deep learning based segmentation technique for dermoscopy images to accurately segment the ROI in the presence of artifacts.

The organisation of the work is mentioned as follows. The related works are represented in Section 2. Section 3 describes the proposed methodology which includes various steps involved in the extraction of precise segmentation. Results and discussion of proposed model for better segmentation outcomes are described under Section 4. Section 5 concludes the proposed method with future scope and references.

2. Related works

Some of the works related to image segmentation are as follows:

Halil and Enes, [16] predicted skin cancer by the processing of skin lesion. The authors used an effective pipeline model to perform lesion segmentation using dermoscopic image. The algorithm used here was the combination of You Only Look Once (YOLO) - grabcut (GC). Four methods were carried out as pre- processing, detection, segmentation and post- processing. The hair on the lesion was removed in the pre-processing phase, the localization of the lesion was determined in the detection phase, the lesion area was divided into different regions in the segmentation stage and post- processing was done with the morphological operators. The method of segmenting the skin lesion in dermoscopic images was estimated based on the familiar datasets as PH2 and ISBI 2017. The detection results achieved in this method were the IOU of 90%, Detection accuracy of 94.40% in PH2 and IOU of 86%, Detection accuracy of 96% in ISBI2017, The limitations in YOLO- grabcut were time consuming and less accurate.

Albahli et al. [17] proposed the method of segmentation of melanoma lesion. The method applied here for the detection of skin cancer was the contribution of YOLO v4 darknet with active contour (AC). In the first step, some of the artifacts which include gel bubbles, hairs, and moles were detached from the images of dermoscopy by the application of morphological operations. Detaching of images was done to sharpen the regions of an image. YOLO v4 detector was used for the melanoma detection to differentiate infected and non-infected areas. The infected regions of melanoma were separated by the application of active contour method. The proposed method of YOLO v4 darknet and active contour was assessed based on the ISIC 2018 and ISIC 2016 datasets. This method gathered the Jaccard coefficient with 0.989 in ISIC 2018 and 0.96 in ISIC 2016.The disadvantages of this method includes the sensitivity and the specificity rate were less.

Ramya et al. [18] offered that detection of malignant melanoma skin cancer by segmentation via automated (CAD). The main attribute of this technique was handling the complexities which include hair follicles, moles, swellings, sweat glands, recognizing the distinct layers by using a discrete wavelet transform. The different stages enhanced in this method were the collection of data, segmentation, and classification of whole image and clearance of surgical margin. The information was gathered from the PH2 dataset and to neglect the unnecessary data, various colour components were analysed by colour spaces such as Ycbcr, HSV. The separation of skin lesion was done by histogram based thresholding. The method of segmentation with discrete wavelet transform was able to acquire the accuracy rate of 86% and sensitivity rate of 91%.The drawbacks in this method were interpretation of human was required and diagnose of the disease was less accurate.

Sikkander et al. [19] suggested the diagnosis of skin lesion on the basis of classification model with segmentation. This model was designed by the combination of adaptive neuro fuzzy classifier (ANFC) model and grabcut algorithm. There were four major steps involved in this method as pre-processing, segmentation, feature extraction and feature classification. In pre-processing stage top hat filter and in-painting technique was carried out. The pre-processed images were segmented by using grabcut algorithm. Feature extraction was worked out by the use of inception model based deep learning. At last, ANFC model is employed to differentiate the images of dermoscopy in to various regions. This method pretends the International Skin Imaging Collaboration (ISIC) dataset. The performance characteristics examined are sensitivity 93.40%, specificity 98.70%, and accuracy 97.91%. The limitations detected in this method were diagnosis of the image did not provide the exact result.

Ozturk and Ozkaya, [20] proposed the segmentation of the skin lesion using (ACNN) adaptive convolutional neural network. To neglect the errors from the data of minute artifacts, an advanced segmentation method which is based on (FCN) fully convolutional network was carried out. The segmentation process using the improved FCN was done without the pre-processing and post- processing stages. This process was done in order to keep up the FCN structure with spatial information. Two contributions were employed to find out the center of the skin lesion and for the clarifications of details about edge. The datasets involved in this method were International symposium on biomedical imaging (ISBI) 2017 and PH2. The performance parameters evolved in the method of segmentation were Jaccard index 78.34%, the mean dice score 88.64% in ISBI 2017 and Jaccard index 87.1%, the mean dice score 93.02% in PH2. The weakness of this model was the Jaccard index value did not meet its requirement.

Kaur et al. [21] offered the process of segmenting the lesion using encoder and decoder methods in modified phase. To overcome the problems of minute artifacts like colour variations, contrast sector and irregular

boundaries, encoder and decoder architecture was employed. This method was highly used to enhance the segmentation process and the details about the infected area were collected. For the calculation of details about artifacts, VGG19 networks weight layers were used. The spatial information of an image was regained through the design of de-convolutional layers. For the better performance of the network, the training parameters which are optimized were adopted. The designed network was evaluated by two datasets as ISIC 2017 and PH2. The performance observations in this method were segmentation accuracy of 95.67%, IOU of 96.70% in ISIC 2017 and accuracy is 98.50 %, IOU of 93.25% in PH2. The drawbacks captured in this model were the outcome of the segmentation precision did not lead to perfection.

Table 1: Analysis of various models for skin cancer detection and segmentation

Author name and reference	Technique used	Objective	Datasets	Performance metrics	Advantages	Disadvantages
Halil and Enes, [16]	YOLO-GC	The processing of skin lesion is carried out by using dermoscopic image.	PH2	Accuracy-94.40 % IOU- 90%	Exact location of the skin lesion can be found.	Detection rate is less Time consumption is high
			ISBI 2017	Accuracy-96% IOU- 86%		
Albahli et al.[17]	YOLOv4 darknet - AC	Segmentation of melanoma is done through morphological operations.	ISIC 2018	Sensitivity-0.93% Jaccard coefficient-0.93	Outcome of morphological operations is effective.	Sensitivity rate is not precise Specificity rate can be better.
			ISIC 2016	Sensitivity-0.94% Jaccard coefficient-0.96		
Ramya et al. [18]	Discrete wavelet transform	Detection of malignant melanoma skin cancer via computer aided diagnosis.	PH2	Accuracy (86%) Sensitivity (91%)	Segmentation of skin lesion is effective.	Human intervention is required Diagnose of disease is challenging
Sikkander et al. [19]	ANFC	Diagnosis of skin lesion is initiated by differentiating the images of dermoscopy.	ISIC	Sensitivity (93.40%) Specificity (98.70%) Accuracy (97.91%)	Feauture extraction of skin lesion is adoptable.	Image diagnosis is not exact
Ozturk and Ozkaya, [20]	FCN	Skin lesion segmentation is undertaken to neglect the	ISBI 2017	Mean jaccard index-78.34% Mean dice score-88.64%	Efficiency of spatial	Ineffective Jaccard value
			PH2	Mean jaccard index-87.1%		

		errors of minute artifacts.		Mean dice score- 93.02%	information is high	
Kaur et al. [21]	Encoder-Decoder	Enhances the skin lesion segmentation by regaining the spatial information	ISIC 2017	Accuracy- 95.67 %	IOU of segmentation is successful	segmentation precision is not perfect
				IOU- 96.70%		
			PH2	Accuracy- 98.50%		
				IOU- 93.25%		
Adegun et al. [22]	FCN	Identification and segmentation of skin lesion through a probabilistic inference approach	ISBI 2017	Accuracy- 97%	Effective mean field is achieved	Error of imperfection
				Dice score - 94%		
			PH2	Accuracy- 96%		
				Dice score - 93%		
Sivanesanet al. [23]	Mask RCNN	Diagnosis of SC by the conversion of synthetic medical images based on extracted edges.	ISIC 2018	Accuracy (90%)	Noise free environment is acquired	Inefficient feature extraction
				Sensitivity (83%)		
				Specificity (94%)		

Adegun et al. [22] suggested a model for the segmentation of the skin lesion in probabilistic model of deep learning. To conquer over the problems of information gathering in artifacts such as hairs blood vessels and skin lines, a probabilistic model was utilized. This model was used to enhance the FCN (Fully convolutional network) based on the deep learning technique. The images of skin lesion was identified and segmented. Probabilistic inference approach was involved for the outcome of effective mean field through the connection with a conditional random field. This process was utilized by the use of Gaussian kernel. At the next step, the skin border lesions were refined for the prediction of skin disease. The skin lesion datasets used for testing the entire framework were ISBI 2017 and PH2. The performance in this model was 97% of accuracy in ISBI 2017 and 96% of accuracy in PH2 for the skin lesion refinement. The drawback in this model was the error occurrence due to the imperfections happened during the skin refinement phase.

Sivanesan et al. [23] offered the early detection of skin cancer using the technique of unsupervised semantic medical image segmentation. The skin lesion was segmented using the edge diagram construction algorithm to reduce the mortality rate. Hence a specific technique for melanoma segmentation called (MRCNN) Mask region based convolutional neural network was implemented. Edge detection method was applied for the synthetic medical image conversion. Based on the extracted edge diagrams, the dataset was constructed with known segmentation by using variations. This model was applied for the early detection of skin lesion and the images of dermoscopy can be diagnosed. The dataset employed here is ISIC 2018 and the approach is checked with the clinical dataset. The efficiency of the segmentation model was evaluated with 90% of accuracy, 83% of sensitivity and 94% of specificity. The limitations faced were the feature extraction was not efficient in this model.

Finally, the authors mentioned above reported that their method paves high detection results, sensitivity rate is efficient, complexity of time is minimized and exact differentiation of artifacts is achieved. But there are certain defects found in these models as there are difficulties to identify the lesion border. Poor performance is achieved when the background of the image touches the boundaries and the discrimination accuracy is difficult. Human intervention is highly required and the sensitivity rate does not meet the requirements. In this work, CAD based deep learning technique for the detection of skin cancer through segmentation process is initiated. This technique acts as the general extension of framework compared to the other methods. The proposed method of segmentation is extremely efficient, consumes lesser computational time, and better generalization capability. Table 1 describes the examination of several models for the detection and segmentation of skin cancer.

3. Proposed Methodology

Skin cancer is one of the major types of cancer in worldwide. The uncontrolled abnormal multiplication of cells causes cancer. The two main reasons for the occurrence of skin cancer are exposure to the harmful ultra-violet rays and the usage of UV tanning beds. This leads to the rapid division of skin cells. Melanoma is the deadliest form of skin cancer and the growth is highly increasing year by year. The origin of melanoma arises from the melanocytes which occur in the form of dark lesion. Due to high similarity, the results of the skin lesion types are diagnosed inaccurately. There are so many challenges in detecting melanoma skin cancer by regretting the noises, improper border lesions and skin lines. Hence, the skin lesion segmentation should be precise in order to detect melanoma. The schematic diagram of proposed methodology is given in figure 1.

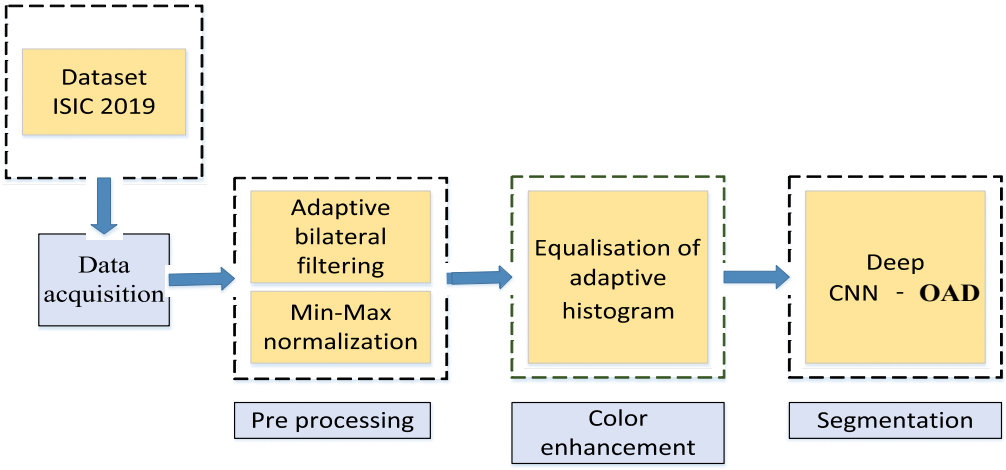

Figure 1: Proposed procedure for melanoma segmentation

The entire process for the detection and segmentation of skin melanoma is shown in Figure 1. A successful technique is implemented in the proposed method, which is represented as the combination of Deep CNN and OAD algorithm. This technique involves four major steps for the better outcome. They are data acquisition, pre-processing, colour enhancement and segmentation.

3.1 Data Acquisition

The dataset used in this technique is International Skin Imaging Collaboration 2019(ISIC 2019). ISIC 2019 is the recent challenging data set which is employed in the proposed model to find out the ability and the accurate classification of melanoma skin lesion. The dataset comprises of 25000 images.For the pre-processing, randomly 9000 images of which 4500 melanoma images are considered and 4500 non-melanoma images are considered. Manual markings are done of those 9000 images to determine the lesion boundaries where ROI(Region of Interest) and NROI(Non-region of interest)portions are identified.Ground truth was created for all the 9000 images. The input images are resized for further processing.

3.2 Pre-processing

The process of improving the quality of a skin lesion image by suppressing various distortions is known as pre-processing. Pre-processing of an image is done to remove all the noise present in the images for obtaining the enhanced output. The refined data of the skin lesion image are collected precisely at this stage. Image normalization is a mode of transformation of input image without degrading the data of an original image. This process is indulged for remodelling the range of pixel intensity values and plays a significant role in pre-processing technique. Normalization of pixel values is proposed for performing the modalities and it does not depend on physical quantities.

By using this, the errors and non-uniformities present in the input image are detached. The best comparison among data acquisition, texture of image can be done and is frequently used for dataset preparation. The input images are similar to the original data which is represented by image function matrix. The images are processed by carrying a single step leading to the elimination of noise. Handling of random errors is much important to bring out the accurate image. Hence pre-processing of an image is done to improve the ability and provide noise free output. By this, the image can be clearly captured and possess the ability to differentiate various types of skin lesions. Thus for an effective image, adaptive method of bilateral filtering is performed.

3.2.1 Adaptive method of bilateral filter

Noise factor is an undesirable feature of a skin lesion image, which gets added at any of the stages during pre-processing and image acquisition. The nature of the noise can either be multiplicative or additive. It affects the pixel's intensity value, which leads to the degradation of image quality. Due to this, the image gets corrupted and results in the faulty diagnosis. Several types of noise gets connected to the images are poisson noise, salt and pepper noise, gaussian noise and speckle noise. Hence for the preferable quality of an image, the removal of noise is done using ABF (Adaptive bilateral filter) method is initiated.

Bilateral filtering (BF) is a technique of low-pass filtering to refine non-iterative and nonlinear data. The main function of BF is image smoothing with edge preservation. The process is done by the replacement of each value of pixel by the average calculation. It depends on two basic parameters as size, contrast and the computational speed can be increased in the larger images. The basic problem of image corruption occurs due to the presence of several noises

BF has high attention to perform filtering of noise in image processing and acts as a smoothing filter for noise reduction. However, the BF technique has several drawbacks that result in noise, inaccurate image results and several types of image artifacts are introduced. Staircase effect and gradient reversal are developed, which represents the false edges of an image. Exact edge detection, edge profile extraction, orientation of edges is difficult and applications of real time can be enhanced based on the availability of network graphics. The performance of BF filter is quite inefficient to remove the higher levels of noise. Hence an adaptive bilateral filtering technique is proposed for the precise output.

To challenge the traditional bilateral algorithm of de-noising, a wavelet – weighted bilateral noise filtering technique is initiated. The noise is suppressed in both high frequency and low frequency domains and the parameters are mentioned as LH (low-high), HL (high-low), HH (high-high) and LL (low-low). The data points are replaced by the weighting points to achieve accuracy of an image. The retaining of edge information in sub-bands of high frequency are given in equations (1) and (2).

$$\mathrm{TH} = \frac{1}{2^{r-1}}\left(w_1 k_1 \sigma_n \sqrt{2 \log Q} + k_2 \frac{\sigma_n^2}{\sigma_{s-r}} \right) \tag{1}$$

From the above equation, standard deviation of noise is denoted as σ_n, standard deviation of noiseless image is denoted by σ_{s-r}, Q represents the total number, TH is the threshold function, the parameters of constant are given as k_1 and k_2, the number of layers is denoted as r and the noise- free signal is mentioned as S.

$$\hat{s} = \begin{cases} 0, & f \le F_r, \\ sign\ (f) \cdot \max\left(|f| - \frac{\sigma_n^2}{P}, 0 \right), & f > F_r, \end{cases} \tag{2}$$

In equation (2), s is the scale parameter; $\hat{s}$ is the estimate of S; and f is the input image. Equations (3) and (4) represents the parameter of noise factor.

$$c(\delta, a) = \exp\left(\frac{\left(\| \delta - a \| \right)^2}{2\sigma_c^2} \right) \tag{3}$$

$$z(f(\delta), f(a)) = \exp\left(\frac{\left(\| \delta - a \| \right)^2}{2\sigma_z^2} \right) \tag{4}$$

In the above mentioned equations, central pixel is denoted as $c(\delta, a)$; $z(\delta, a)$ is denoted as closeness function; the similarity function is given as $z(f(\delta), f(a))$; the standard deviation of the noise is fixed as σ_c and σ_z ; Euclidean distance is denoted by $\|\cdot\|$ and the constant values of σ_c and σ_z are 2.35, 0.1. The assets of wavelet – weighted bilateral noise filtering are the sharpness of image is highly enhanced, image texturing is better, the suitable identification of pixel values, enhancement of high frequency component without eliminating the original data.

3.2.2 Min-Max normalization

It is defined as a scaling or mapping technique to determine a new range from the subsisting range. This technique is enhanced for the purpose of predicting exact result. In this process, the images are resized to a resolution of pixels holding 400×400 these are splitted to a single dataset having the capability to accommodate 4 bytes. A gradient descent version called mini batch is employed to attain the training data over larger datasets. This leads to the process of back propagation individually over various sizes of training dataset and target all the samples of training with same size. This helps in adapting high speed of computation and low memory is required. Eventually, the data is normalized in pre-processing step, which ensures that the mean and the unit variance are zero. Even though the results are improved for noise removal, there is reduced exactness of minute details about the images, the properties of dataset varies and affect the performance of the network. An important issue faced here is the input image can vary the data structure, recognition of image pattern is difficult, and hence a min-max (M-M) normalization technique is employed. Using this, the region with low intensity and high intensity are mapped for the precise output.

The M-M normalisation technique is deployed for contributing linear transformation over the original input image and enhancing the relationship among these data. The details of input image are fixed within a pre-defined boundary for the better outcome. Using this method, the normalized range of data or the values are obtained from the original data which is unstructured. The normalized value can be established by the notion of mean and standard deviation.

Let us consider the original value to be V_o and the normalised value tends to $\hat{V}_o$. The range of V_o can be given as $[\min(V_o), \max(V_o)]$ and the new range is represented as $[\min(V_{new}), \max(V_{new})]$. For the mapping of original value from one range to a new range, the normalised value is given by,

$$\hat{V}_o = \frac{V_o - \min(V_o)}{\max(V_o) - \min(V_o)} (\max(V_{new}) - \min(V_{new})) + \min(V_{new}) \quad (5)$$

Here, the values of $\min(V_{new}), \max(V_{new})$ is set as $(-1,1)$. The strength of M-M normalisation technique is the correlation among the values of original data is maintained. The data redundancy can be diminished and the uprightness is improved.

3.3 Colour enhancement

The skin is composed of different layers and clear review of the lesion is quite demanding. To upgrade the accuracy and resolution of an original image, the process of colour enhancement is accomplished. It is an essential process to neglect the image interferences and provide the visual effects adequately. The enhancement of colouring technique is involved to boost the accuracy, resolution and upgrades the quality of medical image. The exact colour image of the skin lesion produces valuable information about the disease. By the presence of minute artifacts, it adversely affects the appearance of the diagnosed part and results in the outburst of image blurring. The dissimilarities among the normal and abnormal tissue is tough to recognize. Hence, equalisation of adaptive histogram method is launched in order to extract out the image error.

3.3.1 Equalisation of adaptive histogram

Histogram equalisation (HE) is a methodology of image processing, which is able to adjust and improve the colour of an image by the use of histograms. The process is done by broadening the image pixels by considering the intensity values and range. Higher enhancement of colour is accomplished by undertaking this method. It represents the pixel value of image graphically and accumulates the frequencies. Mapping of probability distribution from the input image and extension of dynamic range is put forth to enhance the colour of an overall image. The range of grayscale image is assumed as $[0, r-1]$, holding the gray level as g. The PDF (probability density function) of the input image is denoted as $p_f(f)$. The probability of gray level at k^{th} position is derived as

$$p_f(f_k) = \frac{r_k}{r}, \quad (6)$$

Where, $k = 0, 1, 2, \ldots, g-1$ and f_k represents the k^{th} gray scale. The CDF (cumulative distribution function) $T(f_k)$ is expressed as

$$h = T(f_k) = \sum_{i=0}^{k} p_f(f_i) = \sum_{i=0}^{k} \frac{r_i}{r}, \quad (7)$$

The range of h is given as $0 \le h \le 1$ .The restrictions faced in this method are local contents in the image are not considered, the problems with mean shift are raised, high saturation effects, discrimination is difficult and the calculations are not intensive.The grayscale varies in different regions and the changes made locally in the image are neglected. HE is effectively considered for the particular region and it does not differentiate the bright and dark pixels properly in case of larger regions. To modify these problems, equalisation of adaptive histogram method is accomplished.

Equalisation of adaptive histogram (EAH) is used for the purpose of contrast enhancement by the transformation of gray scale. To reduce the difficulty of noise factor, contrast amplification is limited. The main focus of EAH is to acquire the uniformly distributed intensity levels throughout the scale of intensity. EAH includes several steps of image enhancement processing. The input image is splitted on the basis of two characteristics as regions of continuous and non-overlapping. The size of the region is set as 8×8 . Histogram is evaluated for each region and threshold value for histogram clipping is implemented. The slope of transformation function is limited by the clipping of histogram and the clipped pixel values are distributed uniformly. Local HE is performed on all regions and linear interpolation is initialized for the reconstruction of the pixel value.

Let the assumption be given for the sample point SP as p , the upgraded gray value after interpolation is given as p^{μ}, the sample points are given as $sp_1, sp_2, ..., sp_4$ the mappings of gray level in p are $\delta b_1(p)$, $\delta b_2(p), \delta b_3(p), \delta b_4(p)$ respectively. The upgraded gray value is described by considering the image pixels in three places as edges, corners and at the centre.

The upgraded gray value for the corner image pixels is given as,

$$P^{\mu} = \delta b_1(p) \qquad (8)$$

Where, $\delta b_1(p)$ denotes the gray level mapping of one sample. The upgraded gray value for the edge image pixels is denoted as,

$$p^{u} = (1-\sigma)\delta b_1(p) + \sigma \delta b_2(p) \qquad (9)$$

Where, $(1-\sigma)\delta b_1(p) + \sigma \delta b_2(p)$ denotes the interpolation mapping of two samples. The upgraded gray value for the centre image pixels is denoted as,

$$p^{u} = (1-\alpha)((1-\sigma)\delta b_1(p) + \sigma\delta b_2(p)) + \alpha\,((1-\sigma)\delta b_3(p) + \sigma\delta b_4(p)) \qquad (10)$$

Where, the interpolation mapping of four samples are represented as $(1-\alpha)((1-\sigma)\delta b_1(p) + \sigma\delta b_2(p)) + \alpha\,((1-\sigma)\delta b_3(p) + \sigma\delta b_4(p))$ and α, β are the normalized distances with b_1 .Without any change in hue and saturation, the enhanced image is displayed in RGB colour space by YH inverse transformation. The brightness of the image is re-distributed by calculating several histograms and hence this method is adaptable for the local contrast improvement and edge definition enhancement.

3.4 Segmentation

Segmentation of image gathers a significant role in medical image processing for the determination of affected tumour. By sub-dividing the image into fragmented parts, which are homogeneous in nature, useful details are gathered for predicting an accurate disease. The main aim of this process is to detect the mask of a particular region and contribute semantic interpretation about the level of pixel. This contributes for the understanding of resulted image at higher level and capturing of data is utilized. However, some criteria adversely affects the quality of an image such as locations are not predicted, the size of the partitioned image is irregular, diverse appearances and contrast variations. The generated noise affects the intensity of pixel, resulting in the non-uniformity of tissues and leads to high time consumption. These negativities push the medical image segmentation in to a more challenging section. For promoting precise calculations without losing the original quality of an image, hybrid combination of deep CNN–OAD algorithm is amended.

3.4.1 Deep CNN- OAD

The localisation of skin lesion using segmentation has some of the drawbacks as low contrast problems, lesion boundaries are complex and the lesion shapes are irregular. The actual lesion hold the small area in a larger dermoscopic image and it is difficult to focus on the particular region. Use of Deep CNN faces these drawbacks and acts as the representative neural network with supervised deep learning in the section of image processing and analysing. Skin lesion (SL) localization process is undertaken for placing the lesion in a specific region by not allowing generalization. Segmentation is the crucial step carried out for identifying the infected localisation of skin lesion by separating from the background skin using thresholding. The localization of melanoma SL is characterized and segmented using deep CNN. Figure 2 represents the architecture diagram of different layers in Deep CNN. The proposed deep learning framework for segmentation is given in figure 2.

Deep CNN incorporates encoder and a decoder in the architecture process of output generation. The encoding layers comprises of deep learning of convolution, ReLU, and max pooling. Similarly, decoding layers comprises of deep learning of convolution, ReLU, and max pooling. Finally, output segmented image is obtained by the decision in the final fully connected output layer. By using the effective training data, encoder and decoder works together to reduce the losses. Encoder operation is carried out in the layers of convolution, Rectified linear unit and pooling through the input image. The encoder part is implemented by assembling the down sampling layer and it reduces the spatial resolution of input. The encoded output is fed to the fully connected layer where flattening of samples is generated and by stacking the up sampling layer, the decoder part is constructed and it provides a feature map with low resolution.

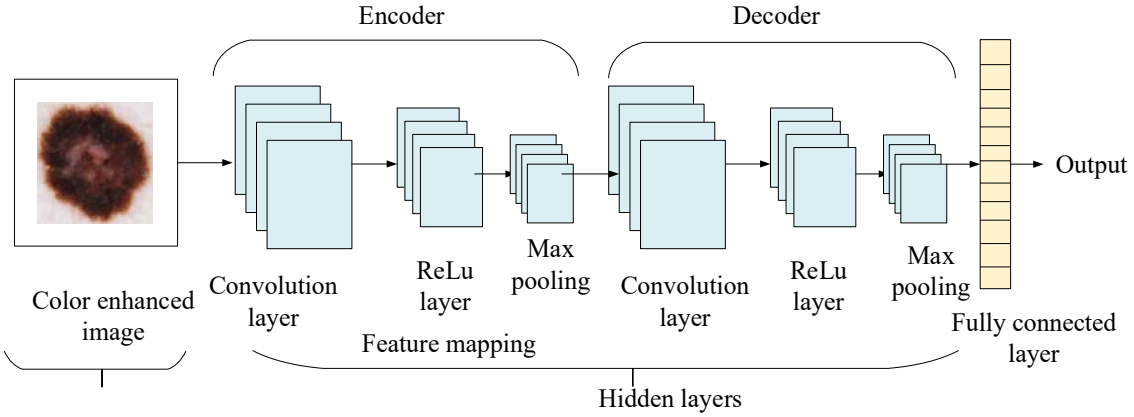

Figure 2: Architecture of proposed Deep learning in segmentation

The medical image of skin lesion is provided in the input layer, convolutional and pooling process is done in the hidden layer to perform the pattern recognition, analysis of spatial data, reduce the dimensions and the number of parameters. The structure is comprised of five layers as input layer, Convolution layer, ReLu layer Pooling layer, fully connected layer and the output layer.

Input layer: The captured image is given as the input and it is represented with pixel intensities. The input layer of a CNN network deals with the artificial neurons and the original data is used for the processing of other following layers. As the input layer consists of first form of data, weights of artificial neurons are calculated in a random manner by transforming to the subsequent layers.

Convolutional layer: The features of an input image are represented in the outline of convolutional layer. In this layer, the original image is filtered from the input and performs a convolution operation. A single value of image is received by the conversion of all the image pixels and the filtered image is passed to the next layer. The updates of back propagation for convolutional layer in a network are derived. In this process, the feature maps from the input layer are put forward to this layer to generate the output feature map. The general notation of convolutional layer is given by;

$$Z_v^l = f\left(\sum_{u \in IN_v} Z_u^{l-1} * m_{uv}^l + ab_v^l\right) \tag{11}$$

Number of input maps selected is given by IN_v, the additive bias for each output map is given by ab, l denotes the number of layers and Z_v^l represents the output of convolution layer, u represents the input map, and v represents the output map.

Rectified linear unit (ReLU): In convolution layer, ReLU is adopted as an activation function due to its superiority. This activation function is responsible for transforming the output to the next layer.

Pooling layer: Pooling layer commences the presence of features in the map provided from convolution. The aim of pooling layer is to transform feature representation in to significant information. Down sampling is an approach which is performed by condensing the existence of features in feature map patches. By using this layer, the dimensions of the image gets reduced, leads to reduction in the number of parameters and the computation. Pooling controls the resolution of feature maps to enhance steadiness in input distortion. The average availability of feature is either detected by average or max pooling layer. They are expressed in the equation (12) and (13).

$$O_{mp} = \max_{(u,v) \in Q_{ab}} Z_{kuv} \tag{12}$$

$$O_{mp} = \frac{1}{\left|R_{mp}\right|} \sum_{(u,v)\in R_{mp}} Z_{kuv} \qquad (13)$$

Where, the size of the pooling region R_{mp} is denoted by $\left|R_{mp}\right|$ .The output of pooling layer is given as O_{mp} , the element within the pooling region R_{mp} at (u, v) is Z_{kuv} . The position which represents the local neighbourhood is (m , p).

Final output layer: The final few layers are formed by the fully connected (FC) layer and the output of pooling layer is given as the input. It is an elementary form of feed forward neural networks and the flattened data are promoted to the FC layer. The overall inputs are attached to every energized unit of the next layer. The data are extracted from the high level features to form the output. The function which denotes the FC layer is given by;

$$Z_{\hat{u}} = \sum_{u} w_{u\hat{u}} x_u + bias_{\hat{u}} \qquad (14)$$

Here, the input given to the FC layer is represented as x, the weight matrix is denoted by w, Z denotes the output and the elements are represented by $u, \hat{u}$.

The output layer accesses the input from previous layers and proceeds with the evaluations for neurons. It is an artificial form of network and the value of output is estimated from the last layer of neurons. The final result produced by the output layer is in the form of refined information with higher detection of accuracy.

The non-linear combinations are processed by flattening the image and given as input to the fully connected layer for the output extraction. Due to the generation of error in the network, the segmented output is compared with the error loss function and exact solution for the evaluation of error rate. Chain rule is initiated to obtain the derivatives of each parameter based on the error rate.

Feed forward is the next step carried out after the parameter updation. This step is repeatedly done till the training of network gets completed. For the activation of neurons, a function of rectified linear unit is initialized as $f(n) = \max(n, 0)$ and to adapt the neuron weight, training error is calculated. The below mentioned formula denotes the cross entropy loss:

$$CE_L = \sum_{u=1}^{P}\sum_{v=1}^{Q} - R_u^{(v)} \log (v)_u^{(v)} \qquad (15)$$

Where, R_u denotes the attained vector of output in m^{th} class, the demanded output vector is given as $R_u = \left(0,...,0,1,...,1,0,...,0\right)$, k implies $1,..., 1$ and the softmax function is implied by the formula given below,

$$(s)_v^{(u)} = \frac{e^{f_u}}{\sum_{v=1}^{Q} e^{f_u}} \qquad (16)$$

The sample number is described as Q and for the function extension, a penalty of weight σ has been added; which is given by,

$$TL = \sum_{u=1}^{P}\sum_{v=1}^{Q} - (v)_u^{(v)} \log (v)_u^{(v)} + \frac{1}{2}\sigma \sum_{K}\sum_{TL} V_{k,tl}^2 \qquad (17)$$

Total number of layers is represented as TL, and k in layer tl indicates the total number of layers and the weight connection is given as v_k .

Adam optimization: CNN is based on tests and errors but, there is existence of some more problems. In recent years, various types of optimal automatic approaches have been presented for extending the network using optimization algorithms. OAD technique is enhanced with deep CNN for solving several problems of segmentation and improving the segmentation accuracy. OAD is a supplement to stochastic gradient descent and it has a broader adoption in the applications of deep learning to perform advanced medical image segmentation. Using this algorithm, the network weights are added iteratively based on the image data.

By merging the characteristics of the adaptive gradient and momentum, hit and trial method is established for determining the adaptive learning rates of each parameter. The moving averages are defined into first and second moments as a_t ,and b_t .

$$a_t = d_1 a_{t-1} + (1-d_1) g_t \quad (18)$$

$$b_t = d_2 b_{t-1} + (1-d_2) g_t^2 \quad (19)$$

Where, the time gradient implies g_t, component wise square is given as g_t^2, the hyper parameters are given as d_1 and d_2, which denotes the exponential decay rate of first and second moment. The estimation value for d_1 and d_2 are set as 0.9, 0.999. The moments are set to 0 initially and are given as $a_0 = b_0 = 0$. Because of the zero initialization, the value is too small for the moving averages and the bias-corrected form is given as:

$$\hat{a}_t = \frac{a_t}{(1 - d_1^t)} \quad (20)$$

$$\hat{b}_t = \frac{b_t}{(1 - d_2^t)} \quad (21)$$

The concluding update for each parameter in a network is given as;

$$\beta_t = \beta_{t-1} - \lambda \frac{\hat{a}_t}{\sqrt{\hat{b}_t} + \theta} \quad (22)$$

Where, the rate of learning is denoted as λ, division of zero is stopped by a very small positive number (θ) and the value is set to 10^{-8}. The value of g_t may comprise both positive and negative components and only positive components are there in g_t^2. All the actions are expressed in the form of component wise. The step size is too small when the gradient transforms its sign frequently and the resulted value of $\hat{a}_t$ might be lower to $\sqrt{\hat{b}_t}$. The estimation of first and second momentum is calculated. The first momentum is achieved by the running average of past gradients which are decaying exponentially and the second momentum is estimated by calculating the square of past gradients.

$$P_{\delta W} = \mu_1 P_{\delta W} + (1-\mu_1) \delta W \quad (23)$$

$$Q_{\delta W} = \mu_2 Q_{\delta W} + (1-\mu_2) \delta W^2 \quad (24)$$

Where, $P_{\delta W}$ and $Q_{\delta W}$ represents the estimation of first and second momentum, μ_1, μ_2 denotes the hyper parameters highlighting the running averages decay. The values of hyper parameters are set to 0.9 and 0.999 respectively. As the running averages of both parameters are influenced by 0, a version of bias correction is evaluated as,

$$P_{\delta W}^{Cor} = \frac{P_{\delta W}}{(1-\mu_1^e)} \quad (25)$$

$$Q_{\delta W}^{Cor} = \frac{Q_{\delta W}}{(1-\mu_2^e)} \quad (26)$$

The recent epoch equals the value of e. At last, the weights are optimized using a weight tensor called W and is derived as;

$$W^{succeeding} = W - \varphi \frac{P_{\delta W}^{Cor}}{\sqrt{Q_{\delta W}^{Cor}} + \omega} \quad (27)$$

To neglect division by zero, the constant term is given as ω which is set to $10^{(-8)}$ and the rate of learning is denoted as φ which is set to 0.0001.

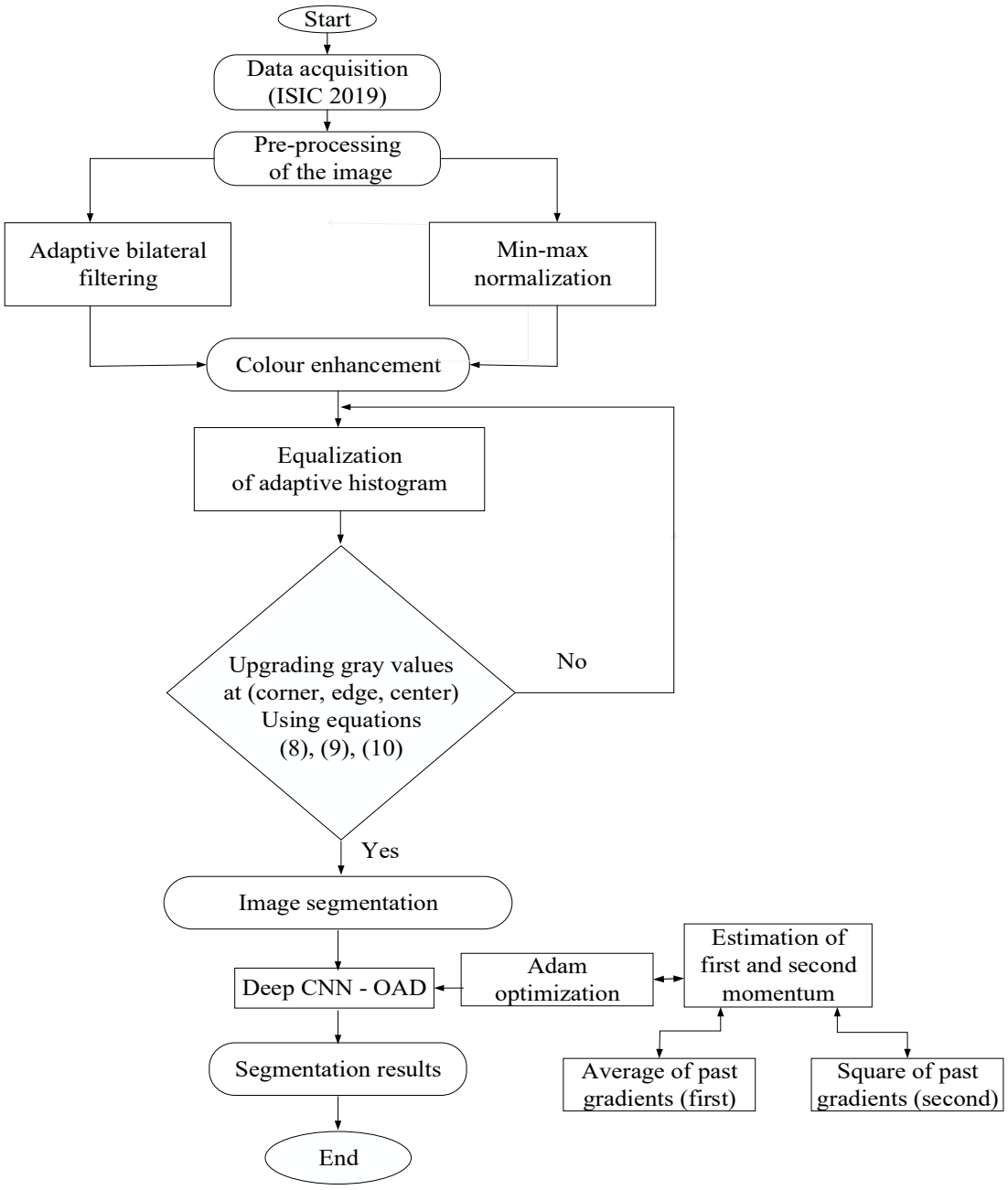

Figure 3: Workflow of the proposed model

The positive properties that are achieved by OAD are the higher computational efficiency, the lower memory requirement, working with large data sets and parameters, the diagonal rescaling of the gradients is invariable and the hyper parameters are interpreted intuitively. Hence, the improvements involved through hybrid combination are location estimation is clear, improves the speed and correctness of border detection, background skin colour estimation is better. This model resulted with great efficiency in the field of image recognition involving visuals of natural and medical for the classification of disease by avoiding the complications. Hence, deep CNN-OAD technique is implemented for the tremendous impact in the field of precise image segmentation process. The work flow of the proposed model is given in figure 3.

Figure 3 describes the workflow for the implementation of Deep CNN-OAD approach. The working procedure for the detection and segmentation of melanoma skin lesions is described in the flowchart. Several steps are undertaken for the effective delivery of segmentation outputs. Initialize the step by acquiring input image data from the ISIC 2019 dataset. The input image may include various noise factors due to the presence of minute artifacts. The first step is to pre-process the input image without losing the details of original image. Two methods are carried out for the removal of noise factor for gathering precise details about the image. Wavelet-weighted bilateral filtering method is deployed in order to remove various noises such as Gaussian, salt and pepper noise.

The normalised range of values is obtained by the contribution of linear transformation in the method of min-max normalization.

The output gained from the pre-processing step is transformed to the colour enhancement process for upgrading the quality of an image. Equalisation of adaptive histogram technique is employed for enhancing the gray values. The pixel intensity of an image is improved by upgrading the gray values at the corner, edge, center using the equations (8), (9), (10). If the values are not upgraded, the process is repeated again with the equalisation of adaptive histogram. If the values are updated, the algorithm is preceded further to the process of image segmentation. For the enhanced segmentation outcomes, the combination of Deep CNN and OAD are performed together. Using Deep CNN, the medical images are classified accordingly and the estimation of first, second momentum is done in OAD. The first momentum is generated by calculating the average of past gradients and the second momentum is evaluated by squaring the past gradients. The deep learning based segmentation approach increased the maximum number of epochs to 100 and reduces the batch size to 10. This is updated to enhance the performance of the segmentation process. At the end of this process, accurate results of segmentation are achieved with better performance.

4. Results and discussion

The experimental results of the proposed skin lesion segmentation using effective deep learning technique are performed in the working platform of MATLAB. The achievement of work by the use of deep CNN-OAD technique is characterized by the use of (CM) confusion matrix. ISIC 2019 is a recent familiar public challenge dataset which is employed to check the capability of proposed method. It works well in the classification of different forms of skin lesion. This dataset comprises of 25,331 images. In total images, 4500 melanoma and 4500 non-melanoma images are selected for the proposed skin lesion segmentation process. By commencing training and testing over the ISIC 2019 dataset will determine the various performance metrics of the proposed method.

4.1 Performance metrics

By comparing previous techniques of skin lesion classification, the performance of proposed method is analysed with different approaches in terms of accuracy, sensitivity, specificity, F1 score, PPV (positive predictive value), NPV (negative predictive value), FPR (false positive rate), FRR (false rejection rate) and FDR (false discovery rate).

4.1.1 Accuracy

The discrimination between a patient and the healthy person in a precise manner is termed as accuracy. For the accurate detection about a person's condition, the cases of true positive and true negative are determined. The derivative form of accuracy can be stated as,

$$\text{Accuracy} = \frac{TP + TN}{TP+TN+FP+FN} \tag{28}$$

Where, (TP) true positive denotes the number of persons who is affected by the disease and the information collected is extremely correct. (TN) true negative represents the number of persons identified exactly as a healthy one and not affected by the disease. (FP) false positive defines the number of persons who is wrongly identified as they are affected by the disease. (FN) false negative represents the number of persons who is incorrectly considered as they not affected by any disease.

4.1.2 Sensitivity

The information is said to be highly sensitive if it has the capacity to establish the positive cases of patients accurately. The proportion of TP in patient cases should be calculated for the estimation of sensitivity. It is denoted by the following equation:

$$\text{Sensitivity} = \frac{TP}{TP + FN} \tag{29}$$

4.1.3 Specificity

Specificity is defined as the ability to correctly discover healthy person who are not affected by any disease. To estimate the specificity, the proportion of participants should be determined in different person and is derived as:

$$\text{Specificity} = \frac{TN}{TN + FP} \tag{30}$$

4.1.4 F1 score

The harmonic mean between precision and recall is defined as the F1 score. The performance can be rated by using this as a statistical measure and is derived as:

$$F1\ score = \frac{TP}{TP + \frac{1}{2}(FP + FN)} \tag{31}$$

4.1.5 PPV (Positive predictive value)

The probability which denotes the detection of disease with a positive screening test is defined as PPV and the estimation is given by,

$$PPV = \frac{TP}{(TP + FP)} \tag{32}$$

4.1.6 NPV (Negative predictive value)

The probability which denotes the non-detection of disease with a negative screening test is defined as NPV and the estimation is given by,

$$NPV = \frac{TN}{(TN + FN)} \tag{33}$$

4.1.7 FRR (False rejection rate)

The probability which defines the measure of correct acceptance is defined as FRR. The ratio between the number of genuine asserts to the accesses provides the FRR value and is described as,

$$FRR = \frac{FN}{FN + TP} \tag{34}$$

4.1.8 FDR (False discovery rate)

FDR determines the probability of type of errors in null testing and it includes both the false and true positives. FDR can be estimated by,

$$\text{FDR} = \frac{FP}{TP + FP} \tag{35}$$

4.1.9 FOR (False omission rate)

FOR calculates the proportion of false negatives which are declined wrongly and it is referred as the complement to the NPV. FOR is denoted by the following equation,

$$FOR = \frac{FN}{FN + TN} \tag{36}$$

4.1.10 TS (Threat score)

Threat score defines the performance prediction of total number of correct events to the total number of missed events. TS is also mentioned as critical success index.

$$TS = \frac{TP}{TP + FN + FP} \tag{37}$$

4.2 Performance analysis

The exact guidance is achieved by providing an ideal performance analysis in all cases. The significant data is collected to evaluate the current performance using several performance metrics. Ten features are quantitatively calculated such as accuracy, sensitivity, specificity, F1 score, PPV, NPV, FRR, FDR, FOR, TS and the predictive performance is analysed by the implementation of this process.

Table 2: Results of proposed work in terms of different performance metrics

Samples	Accuracy	Sensitivity	Specificity	F1 score	PPV	NPV
1	0.90	0.76	0.97	0.83	0.93	0.89
2	0.98	0.96	0.98	0.97	0.97	0.98
3	0.85	0.60	0.97	0.73	0.92	0.84
4	0.90	1	0.89	0.56	0.39	1
5	0.98	0.94	0.99	0.96	0.98	0.98
6	0.93	0.83	0.97	0.87	0.92	0.93
7	0.96	0.92	0.98	0.94	0.96	0.96
8	0.95	0.99	0.95	0.87	0.77	0.99
9	0.89	0.78	0.97	0.86	0.96	0.86
10	0.95	0.99	0.94	0.86	0.76	0.99
11	0.96	0.92	0.98	0.95	0.97	0.95
12	0.92	0.95	0.90	0.87	0.80	0.97
13	0.96	0.95	0.96	0.93	0.91	0.98
14	0.88	0.95	0.85	0.83	0.74	0.97
15	0.98	0.96	0.98	0.95	0.94	0.99
16	0.91	0.85	0.98	0.91	0.97	0.86
17	0.96	0.96	0.97	0.95	0.95	0.97
18	0.95	0.89	0.98	0.93	0.96	0.94
19	0.93	0.86	0.98	0.91	0.97	0.91
20	0.98	0.98	0.98	0.96	0.94	0.99
Mean	0.94	0.89	0.96	0.88	0.89	0.95

Table 3: Output performances for the proposed method in FRR, FDR, FOR, TS

Samples	FRR	FDR	FOR	TS
1	0.02	0.06	0.10	0.72
2	0.01	0.02	0.01	0.94
3	0.02	0.07	0.15	0.57
4	0.10	0.60	0	0.39
5	0.00	0.01	0.01	0.93
6	0.02	0.07	0.06	0.77
7	0.01	0.03	0.03	0.90
8	0.04	0.22	0.00	0.77
9	0.02	0.03	0.13	0.76
10	0.05	0.23	0.00	0.75
11	0.01	0.02	0.04	0.90
12	0.09	0.19	0.02	0.77
13	0.03	0.08	0.01	0.87
14	0.14	0.25	0.02	0.72
15	0.01	0.05	0.00	0.91
16	0.01	0.02	0.13	0.83
17	0.02	0.04	0.02	0.92
18	0.01	0.03	0.05	0.87
19	0.01	0.02	0.08	0.84
20	0.01	0.05	0.00	0.92
Mean	0.03	0.04	0.79	0.89

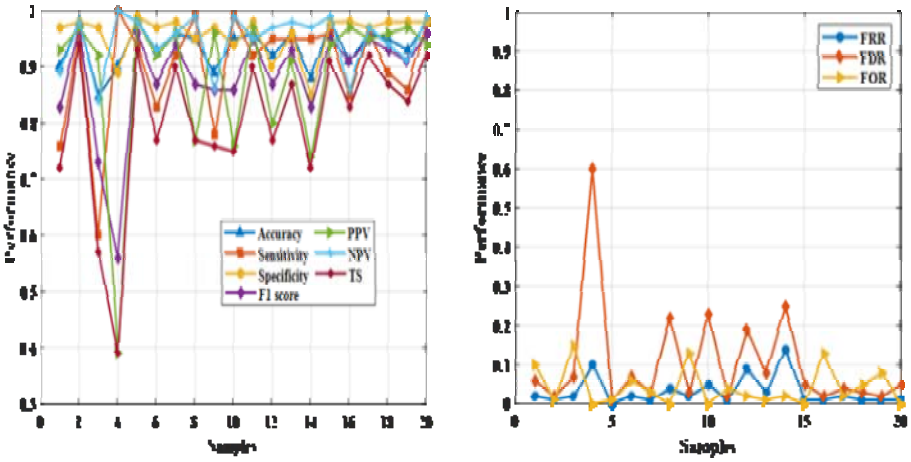

Figure 4: Comparison of output performance

Table 2 presents the mean value of various terms where a set of twenty different samples are given as the input. These sample images are processed with several steps for the estimation of correct result. The calculation is done by considering different terms as accuracy, sensitivity, specificity, F1 score, PPV and NPV. The mean accuracy of melanoma skin lesion segmentation provides 0.94, the sensitivity rate is attained as 0.89, specificity rate prolongs to 0.96, F1Score achieved 0.88 of output, PPV and NPV rates are generated as 0.89 and 0.95.

Table 3 proposes the estimation of mean value by implementing various terms such as FRR, FDR, FOR, TS. The input image consist of 20 samples are given as the input for evaluating different performance output. The outcome of FRR with respect to different samples are given as 0.03, FDR provides 0.04 of output, FOR and TS leads to 0.79, 0.89 as a result of segmentation.

Figure 4 represents the comparison of output performance by considering various samples. A set of twenty samples are considered for evaluating the overall performance. In contrast with the different performance metrics, the mean value of each sample is obtained and the results are shown graphically. The mean values obtained for the twenty samples in terms of accuracy as 0.94, sensitivity as 0.89, specificity as 0.96, F1 score as 0.88, PPV as 0.89, NPV as 0.95, FRR as 0.03, FDR as 0.04, FOR as 0.79 and TS as 0.89. Table 4 depicts the comparison of proposed deep CNN-OAD performance.

Table 4: Comparison of proposed Deep CNN-OAD performance

Technique	**Dataset**	**Performance metrics**		
		Accuracy	**Sensitivity**	**Specificity**
Deep CNN-OAD (Proposed method)	**ISIC 2019**	**0.9406**	**0.89**	**0.96**
YOLO v4 darknet and active contour (AC) [17]	ISIC 2018	0.93	0.94	0.95
YOLO – grabcut(GC) [16]	PH2	0.94	0.83	0.94
Discrete wavelet transform [18]	PH2	0.86	0.91	-
Mask RCNN [23]	ISIC 2018	0.90	0.83	0.94

Figure 5 represents various techniques deployed in the process of image segmentation for the exact clarification about the disease. The current work using Deep CNN- OAD has achieved 94.06% of accuracy in skin cancer detection and segmentation. The result of existing performance in melanoma detection through segmentation in the combinational approach of YOLO v4 darknet and active contour has achieved an accuracy of 93%. Through YOLO-GC algorithm achieves 94% of accuracy in lesion location and segmentation. Using discrete wavelet transform, accuracy is 86% in the process of segmentation via CAD. Unsupervised semantic medical image segmentation provides 90% of accuracy in the technique of Mask RCNN. Comparing the rate of accuracy with the existing approaches, it clearly shows that the performance of proposed method in Deep CNN-OAD is reasonably better in the process of segmentation.

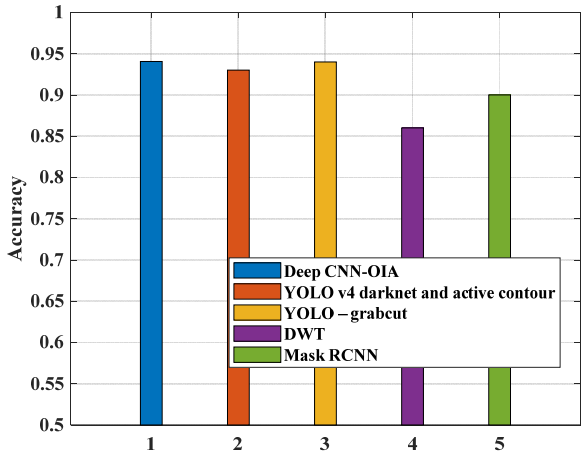

Figure 5: Accuracy Comparison

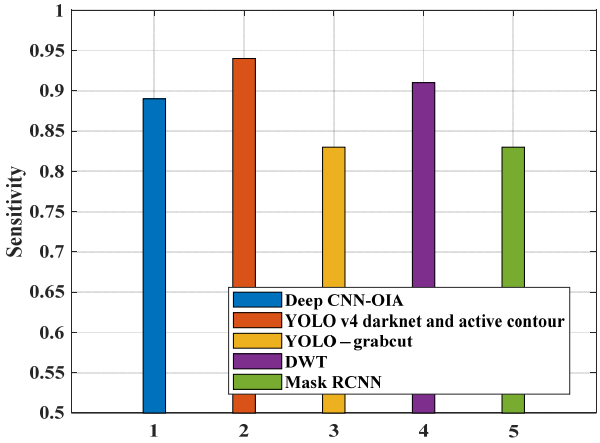

Figure 6: Sensitivity Comparison

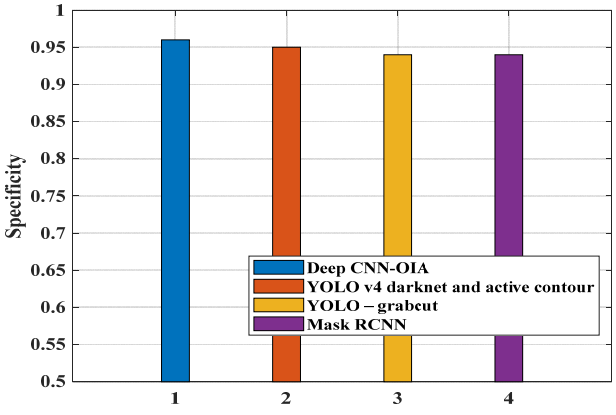

Figure 7: Specificity Comparison

The proposed effort in the combination of Deep CNN and OAD obtained sensitivity of 89.43% is shown in Figure 6. The rate of sensitivity for the previous approaches is mentioned in the comparison field. 94% of sensitivity is gained through the technique of YOLO v4 darknet and active contour. Both of the YOLO-GC algorithm and Mask RCNN attains the sensitivity rate as 83% in segmenting the image for exact findings. 91% of positive rate is gathered by the approach of unsupervised semantic medical image segmentation.

In Figure 7, the specificity rate for the proposed method in Deep Convolutional neural network and optimization of improved Adam is 96%. The models which include Mask RCNN, YOLO-GC algorithm gathers 94% as the rate of specificity in lesion partitioning and semantic segmentation of medical imaging. 95% is obtained as the specificity rate for the detection of melanoma in the technique of YOLO v4 darknet and active contour.

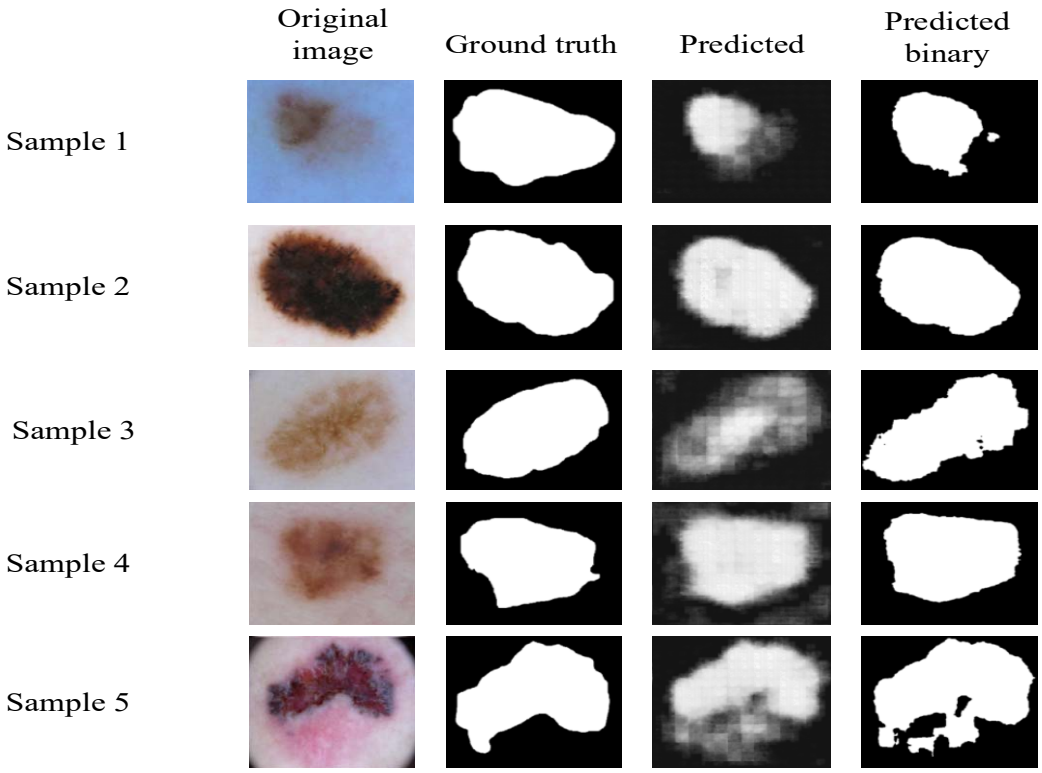

Figure 8: Segmentation outcomes

Figure 8 shows the outcome of segmentation results by representing five samples. A set of twenty samples are obtained for the clarification and prediction of exact result. In each sample, a different skin lesion image is given as the input for the detection of melanoma. The original image consists of various noises which leads to inaccurate results. To conquer this problem, the noise is removed by collecting clear information about the disease without losing the qualities of original image. Precise segmentation results are gathered by obtaining the output of ground truth, predicted and predicted binary forms.

5. Conclusion

A dominant technique is presented in the proposed method for pre-processing, enhancement of colour and segmentation of skin lesion using Deep CNN-OAD. With this architecture, the segmentation problem in identifying the particular lesion is overcome by reducing the computational complexity and achieves better result without deterioration in the original input. In contrast with the work of existing approaches, the resulted efficiency is comparatively higher in the proposed work. The achievements in the results of segmentation are measured through various performance metrics such as accuracy (94%), sensitivity (89%), Specificity (96%), F1 score (88%), PPV (89%), NPV (95%), FRR (3%), FDR (4%), FOR (79%) and TS (89%). The previously used algorithms such as YOLO v4 darknet-AC method attained (93%) of accuracy, discrete wavelet transform achieved (86%) of accuracy with PH2 dataset and the technique of Mask RCNN acquired (90%) of accuracy with ISIC 2018 dataset. The performance metrics comparison on previous approaches, the proposed Deep CNN-OAD accumulated (94.06%) of accuracy with the training of ISIC 2019 dataset. As the data are collected from a single dataset, the exact segmentation results may lag. The upcoming work can be improved further to detect melanoma SC efficiently with high accuracy. Additional enhancement can be done by gathering more information from various datasets and the segmentation method can be modified for the more reliable outcome.

Funding
No funding is provided for the preparation of manuscript.

Conflicts of interest

The authors have no conflicts of interest to declare.

References

[1] Leiter, U.; Keim, U.; Garbe, C. (2020). Epidemiology of skin cancer: update 2019. *In Sunlight, Vitamin D and Skin Cancer, Springer, Cham*, pp. 123-139.
[2] Lippert, T.P.; Greenberg, R.A. (2021). The abscopal effect: a sense of DNA damage is in the air. *Journal of Clinical Investigation* **131**(9), pp. e148274.

[3] Sarangapany, T.; Darmanayagam, S.E.; Rajamanickam, P.; Raj, S.R. (2021). An Enhanced Approach for Skin Lesion Smoothening and Segmentation from Dermoscopic Images. *Solid State Technology* **64**(2), pp. 2645-58.
[4] Jones, O.T.; Ranmuthu, C.K.; Hall, P.N.; Funston, G.; Walter, F.M. (2020). Recognising skin cancer in primary care. *Advances in therapy* **37**(1), pp. 603-16.
[5] Kawaguchi, M.; Kato, H.; Tomita, H.; Hara, A.; Suzui, N.; Miyazaki, T.; Matsuyama, K.; Seishima, M.; Matsuo, M. (2020). Magnetic resonance imaging findings differentiating cutaneous basal cell carcinoma from squamous cell carcinoma in the head and neck region. *Korean journal of radiology* **21**(3), pp. 325-31.
[6] Zghal, N.S.; Derbel, N. (2020). Melanoma skin cancer detection based on image processing. *Current Medical Imaging* **16**(1), pp. 50-8.
[7] Ningrum, D.N.; Yuan, S.P.; Kung, W.M.; Wu, C.C.; Tzeng, I.S.; Huang, C.Y.; Li, J.Y.; Wang, Y.C. (2021). Deep Learning Classifier with Patient's Metadata of Dermoscopic Images in Malignant Melanoma Detection. *Journal of Multidisciplinary Healthcare* **14**, pp. 877.
[8] Senan, E.M.; Jadhav, M.E. (2021). Analysis of dermoscopy images by using ABCD rule for early detection of skin cancer. *Global Transitions Proceedings*. **2**(1), pp. 1-7.
[9] Khan, A.H.; Iskandar, D.N.: Al-Asad, J.F.: El-Nakla, S. (2021). Classification of skin lesion with hair and artifacts removal using black-hat morphology and total variation. *International Journal of Computing and Digital Systems* **10**, pp. 597-604.
[10] Singh, L.; Janghel, R.R.; Sahu, S.P. (2021). Automated CAD System for Skin Lesion Diagnosis: A Review. *Advances in Biomedical Engineering and Technology* pp. 295-320.
[11] Khan, M.A.; Sharif, M.; Akram, T.; Damaševičius, R.; Maskeliūnas, R. (2021). Skin lesion segmentation and multiclass classification using deep learning features and improved moth flame optimization. *Diagnostics*. **11**(5), pp. 811.
[12] Araújo, R.L.; de Andrade, L.R.R.; Rodrigues, J.J.; e Silva, R.R. (2021). Automatic Segmentation of Melanoma Skin Cancer Using Deep Learning. *In 2020 IEEE International Conference on E-health Networking, Application & Services (HEALTHCOM)* pp. 1-6.
[13] Barata, C.; Celebi, M.E.; Marques, J.S. (2018). A survey of feature extraction in dermoscopy image analysis of skin cancer. *IEEE journal of biomedical and health informatics* **23**(3), pp. 1096-109.
[14] Taufiq, M.A.; Hameed, N.; Anjum, A.; Hameed, F. (2017). m-Skin Doctor: A mobile enabled system for early melanoma skin cancer detection using support vector machine. *IneHealth 360°. Springer, Cham* pp. 468-475.
[15] Abbes, W.; Sellami, D.; Marc-Zwecker, S.; Zanni-Merk, C. (2021 Apr 18). Fuzzy decision ontology for melanoma diagnosis using KNN classifier. *Multimedia Tools and Applications* pp.1-22.
[16] Ünver, H.M.; Ayan, E. (2019). Skin lesion segmentation in dermoscopic images with combination of YOLO and grabcut algorithm. *Diagnostics* **9**(3), pp. 72.
[17] Albahli, S.; Nida, N.; Irtaza, A.; Yousaf, M.H.; Mahmood, M.T. (2020 Nov 3). Melanoma lesion detection and segmentation using YOLOv4-DarkNet and active contour. *IEEE Access* **8**, pp.198403-14.
[18] Ramya, J.; Vijaylakshmi, H.C.; Saifuddin, H.M. (2021). Segmentation of skin lesion images using discrete wavelet transform. *Biomedical Signal Processing and Control* **69**, pp. 102839.
[19] Sikkandar, M.Y.; Alrasheadi, B.A.; Prakash, N.B.; Hemalakshmi, G.R.; Mohanarathinam, A.; Shankar, K. (2021). Deep learning based an automated skin lesion segmentation and intelligent classification model. *Journal of ambient intelligence and humanized computing* **12**(3), pp. 3245-55.
[20] Öztürk, Ş.; Özkaya, U. (2020). Skin lesion segmentation with improved convolutional neural network. *Journal of digital imaging* **33**(4), pp. 958-70.
[21] Kaur, R.; Hosseini, H.G.; Sinha R. (2021). Deep Learning in Medical Applications: Lesion Segmentation in Skin Cancer Images Using Modified and Improved Encoder-Decoder Architecture. *Geometry and Vision*. **1386**, pp. 39.
[22] Adegun, A.A.; Viriri, S.; Yousaf, M.H. (2021). A Probabilistic-Based Deep Learning Model for Skin Lesion Segmentation. *Applied Sciences* **11**(7), pp. 3025.
[23] Sivanesan, U.; Braga, L.H.; Sonnadara, R.R.; Dhindsa, K. (2019). Unsupervised medical image segmentation with adversarial networks: From edge diagrams to segmentation maps. *arXiv preprint arXiv:1911.05140*.

Authors Biography

Ramandeep Kaur, she is currently Pursuing PhD at Sri Guru Granth Sahib World University. Also, working as a Lecturer at Government College for Girls, Patiala. She obtained her B.C.A degree from Punjab Technical University, Jalandhar in 2010 and she pursued her M.C.A degree from Punjabi University, Patiala in 2013.

Dr. Navdeep Kaur is a Professor in the Department of Computer Science at Sri Guru Granth Sahib World University, Fatehgarh Sahib, Punjab, India. She received her B.Tech degree in 1997, M.Tech degree in Computer Science and Engineering from Kurukshetа University in 1998 and Ph.D degree in Computer Science and Engineering from IITR, Roorkee in 2008.
She has published over 100 peer-reviewed papers in reputed international journals and conferences. Her current research interests include cloud computing, Information security, sensor networks and machine learning. She has graduated 9 Ph.Ds (currently working with another 8 Ph.D students).